

Experimental and quantum chemical studies of anionic analogues of N-heterocyclic carbenes

Received 00th January 20xx,
Accepted 00th January 20xx

DOI: 10.1039/x0xx00000x

www.rsc.org/

Haoyu Niu,^a Robert J. Mangan,^a Andrey V. Protchenko,^a Nicholas Phillips,^a Wiebke Unkrig,^a Christian Friedmann,^a Eugene L. Kolychev,^a Rémi Tirfoin,^a Jamie Hicks^a and Simon Aldridge*^a

A combination of quantum chemical and synthetic/crystallographic methods have been employed to probe electronic structure in two series of anionic ligands related to the well known N-heterocyclic carbene (NHC) class of donor. Analyses of (i) the respective frontier orbital energies/compositions for the 'free' ligands and the results of ETS-NOCV studies of the bonding in model group 11 complexes; and (ii) the structural metrics for (new) linear gold(I) compounds, have been used to probe the bonding in complexes of NHC ligands which incorporate a backbone-appended weakly-coordinating anion component (WCA-NHCs) and in systems featuring the isoelectronic (formally anionic) diazaborolyl ligand family. Key findings are that WCA-NHC ligands – in which the anionic component is attached to the ligand heterocycle via a methylene (CH₂) spacer – offer electronic (and steric) properties which are largely unperturbed from their 'simple' NHC counterparts, while diazaborolyl donors (in which the negative charge is formally located at the boron donor atom) offer significantly stronger σ -donation and a very high *trans* influence.

Introduction

N-heterocyclic carbenes (NHCs; e.g. **I**, Figure 1) are neutral, carbon-donor ligands which have been widely exploited in the stabilization of cationic metal species implicated in homogeneous catalysis.^{1,2} They are known to be very strong σ -donors, and the strong metal-ligand bonds formed with late transition metal centres underpin the longevity of many 'Noble' metal NHC catalysts.²

For the isolation of free (i.e. uncomplexed) NHCs, so-called 'push-pull' electronic stabilization is known to be a significant enabling factor; inductive stabilization of the HOMO and mesomeric destabilization of the LUMO by the electronegative and π -donor α -nitrogen substituents typically contribute to a relatively wide HOMO-LUMO separation.³ More recently, expanded ring NHC systems (**II**) and cyclic amino alkyl carbenes (cAACs, **III**) have been explored,^{4,5} demonstrating how the HOMO and LUMO energies (and consequently ligand properties) can be tuned by heterocycle design.

Anionic variants of NHCs featuring a pendant weakly-coordinating anion component tethered to the heterocycle backbone (WCA-NHCs) have recently emerged (e.g. **IV**), in part driven by a desire to generate zwitterionic metal complexes with improved solubility in apolar media.^{6,7} Such systems have been shown to be effective, for example, in bringing about catalytic hydrogenation chemistry in pure hydrocarbon

media.^{7b} We have been interested in expanding the scope of such systems, by developing versatile synthetic routes to a range of WCA-NHC complexes offering systematic variation in the size of the heterocyclic backbone (e.g. **V**, where $m = 1-3$).⁸ For systems of this type, we hypothesized that the remote CH₂-mediated tethering of the WCA component (*cf.* direct bonding to the ligand heterocycle in systems of type **IV**)⁷ should give rise to relatively unperturbed ligand properties closely aligned with those of the corresponding 'simple' NHCs.

A related class of complex are those containing diazaborolyl ligands (**VI**), based on an isoelectronic B-containing heterocycle with the anionic charge formally localized at boron. Compounds containing such ligands have been known since the 1990s,^{9,10} but recent syntheses owe much to the development of nucleophilic boryllithium reagents by Yamashita, Nozaki and co-workers in 2006.¹¹ Superficially, diazaborolyl ligands have a similar frontier orbital make up to NHCs, *i.e.* a boron lone-pair type HOMO, and a LUMO potent-

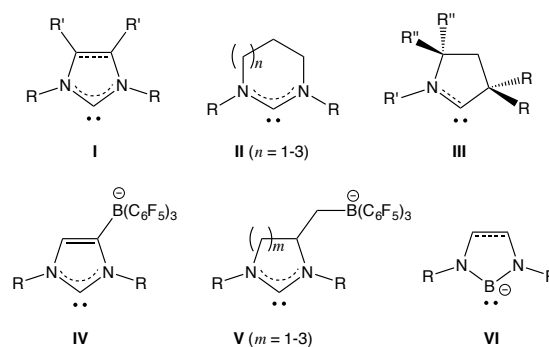


Figure 1 Neutral NHC and isoelectronic (anionic) boryl ligands.

^a Department of Chemistry, University of Oxford, Inorganic Chemistry Laboratory, South Parks Road, Oxford, UK. OX1 3QR. E-mail: Simon.Aldridge@chem.ox.ac.uk
Electronic Supplementary Information (ESI) available: additional synthetic and characterizing data; details of DFT calculations; CIFs for all crystal structures. See DOI: 10.1039/x0xx00000x

ially featuring a significant contribution from the perpendicular B p_{π} orbital.¹² Observations made from structural studies of *p* and *d*-block systems, however, imply that these B-donor ligands present an even higher degree of σ electron donation than do NHCs.¹³

Given our ongoing interests in both of these families of anionic ligands,^{8,14} and their relationships to the widely-used NHC donor class, we perceived the need for a systematic study – involving both structural and quantum chemical input – of their comparative ligand properties. Our efforts in this direction are summarized below.

Results and discussion

(i) Quantum chemical analyses of "free" ligands

Ligand selection and optimization

Figure 2 shows the carbene and diazaborolyl ligands which have been probed in the current study. These can be subdivided into neutral N-heterocyclic carbenes (NHCs) (Figure 2, left column, denoted by the label c), N-heterocyclic carbenes incorporating a pendant weakly coordinating anion component (WCA-NHCs) (centre, labelled c'), and formally anionic diazaborolyl ligands (right, labelled b). In each case the prefix denotes the nature of the central heterocycle, be it imidazole (I-) or benzimidazole-derived (B-), or based on a saturated 5-, 6- or 7-membered core (5-, 6-, 7-); the nature of the N-bound aryl group is indicated by the superscript tag.

Isolable NHCs, of course, have been known for many years, as outlined above,¹ and their experimental properties are well understood. We therefore sought to use these systems as a computational baseline for our subsequent analyses of the electronic structure in less familiar WCA-NHC and diazaborolyl systems.³ As such, the perturbation brought about by introducing a pendant borate functionality, or by formally replacing the carbene carbon with boron, could readily be assessed for a range of

heterocyclic systems. In all cases, calculations were carried out on systems featuring mesityl groups as the N-aryl substituents (although some experimental studies rely on bulkier Dipp groups). This regime was employed in order to provide uniform like-for-like comparison between the different classes of ligand, without unduly expanding the computational timeframe of the study.

Geometry optimisations were first carried out on ligands for which experimental crystallographic data were available, with the key results being displayed in Table 1. In general, the agreement

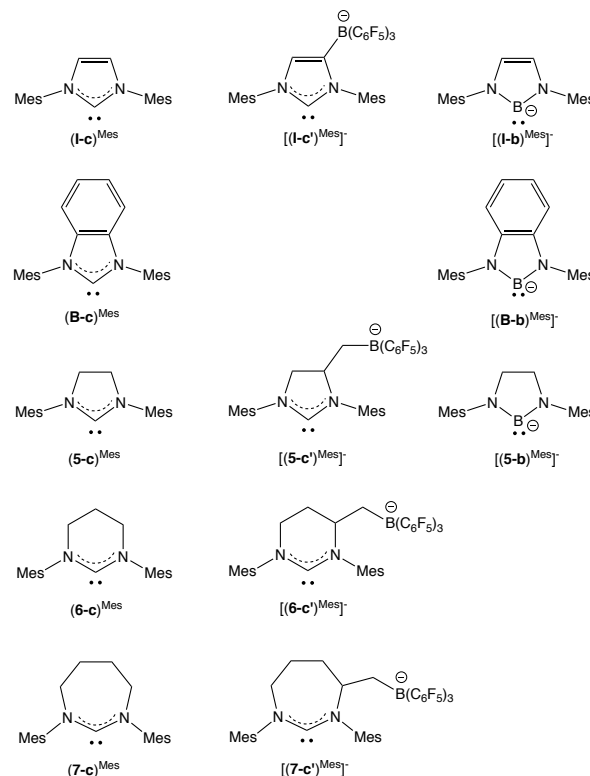


Figure 2 NHC, WCA-NHC and boryl ligands examined in the current study

Table 1 Key geometric parameters for (I-c)^{Mes}, (5-c)^{Mes}, (6-c)^{Mes}, (7-c)^{Mes}, [(I-c')^{Mes}][⁻], [(5-c')^{Mes}][⁻] and [(I-b)^{Mes}][⁻] derived from X-ray crystallography and DFT calculations.

Ligand	Ref	Experimental			Calculated		
		N-C(B)-N bond angle (°)	N-C(B) bond length (Å)	C-C 'backbone' separation (Å) ^a	N-C(B)-N bond angle (°)	N-C(B) bond length (Å)	C-C backbone distance (Å) ^a
(I-c) ^{Mes}	15	101.4(2)	1.371(4)	1.333(5)	101.2	1.375	1.361
(5-c) ^{Mes}	16	104.7(3)	1.352(5)	1.505(6)	105.8	1.350	1.531
(6-c) ^{Mes}	4a	114.7(1)	1.346(1)	2.453(2)	115.3	1.350	2.485
(7-c) ^{Mes}	4a	116.6(4)	1.346(5)	2.787(6)	117.5	1.351	2.836
[(I-c') ^{Mes}] [⁻]	7b	102.2(1)	1.363(1), 1.368(1)	1.357(1)	101.3	1.371, 1.378	1.364
[(5-c') ^{Mes}] [⁻] ^b	8	104.7(2)	1.353(3), 1.353(4)	1.514(4)	105.5	1.350, 1.354	1.537
[(I-b) ^{Mes}] [⁻] ^b	11c	98.6(2)	1.474(4), 1.481(4)	1.338(4)	97.7	1.483	1.363
[(5-b) ^{Mes}] [⁻] ^c	11b	101.9(2)	1.455(2)	1.524(2)	101.5	1.459	1.534

^a Defined as the distance between the two backbone carbon atoms attached to nitrogen. ^b Experimental data for the N-Dipp analogue, as [K(18-crown-6)]⁺ derivative; calculated data for [K(thf)₃]⁺ system. ^c Experimental data for the N-Dipp analogue, as [Li(thf)₂]⁺ derivative; calculated data for N-Mes, [Li(thf)₂]⁺ system.

between the calculated and measured metrical parameters is very good. Thus, for example, differences in the key N-C-N bond angle are small: the calculated value for $(\mathbf{5-c})^{\text{Mes}}$ diverges by 1.1° ,¹⁶ but the remainder all have discrepancies of less than 1° . In the case of the WCA-NHC and boryl systems, the most convenient experimentally determined solid-state metrical data for the 'isolated' anions are derived from adducts featuring Group 1 metal cations. Thus, the complexes of $[(\mathbf{5-c}')^{\text{Mes}}]^-$ (or strictly its N-Dipp substituted analogue) with $[\text{Li}(\eta^6\text{-toluene})]^+$ and $[\text{K}[18\text{-crown-6}]]^+$ have been crystallographically characterized,⁸ as have $[\text{Li}(\text{thf})_2]^+$ complexes of $[(\mathbf{I-b})^{\text{Dipp}}]^-$ and $[(\mathbf{5-b})^{\text{Dipp}}]^-$.^{11b,c} Thus, model systems featuring $[(\mathbf{5-c}')^{\text{Mes}}]^-$ and $[(\mathbf{I-b})^{\text{Mes}}]^-$ complexed to $[\text{Li}(\text{thf})_2]^+$ and $[\text{K}(\text{thf})_3]^+$ were optimized computationally and the metrical parameters compared to the available experimental data (Table 1). Here too, agreement between the two sets of data was very good.

From a geometric perspective, a key parameter relating to the σ -donor properties of all three classes of ligand is the N-E-N angle ($E = \text{C}, \text{B}$),^{1,3} and this metric is very well modelled computationally. In general, both N-C-N and N-B-N angles increase as the heterocyclic backbone increases in size: for saturated NHCs and WCA-NHCs the N-C-N angle widens with increasing length of the hydrocarbon linker between the two nitrogen atoms (i.e. from 5- to 6- to 7-membered heterocycles). More subtly, N-E-N angles also widen on going from systems featuring unsaturated backbones (e.g. $(\mathbf{I-c})^{\text{Mes}}$) to saturated linkers (e.g. $(\mathbf{5-c})^{\text{Mes}}$); this reflects the increase in the backbone C-C bond length as the formal bond order changes from two to one. Boryl systems typically feature narrower N-E-N angles than their NHC analogues, reflecting the larger covalent radius of boron within otherwise similar heterocycle frameworks.¹⁶

Electronic structure

Table 2 lists the calculated energies of the σ and p_π orbitals for each of the ligands, both in the gas phase and with allowance made for the thf dielectric effect using the COSMO approach. With the exception of the benzannulated systems (i.e. $(\mathbf{B-c})^{\text{Mes}}$ and $[(\mathbf{B-b})^{\text{Mes}}]^-$), the calculated data for NHC, WCA-NHC and boryl ligands follow a common trend: widening of the N-C-N bond angle (e.g. by expanding the heterocycle), leads to a reduction in the s:p ratio (greater p character) and a consequent increase in the energy of the σ orbital (HOMO).^{1b} The energy of the p_π orbital is less sensitive to these geometric changes, with the effect that the σ - p_π energy separation systematically falls. With respect to the NHC and WCA-NHC systems, the change is most marked between the saturated five-membered systems $(\mathbf{5-c})^{\text{Mes}}/[(\mathbf{5-c}')^{\text{Mes}}]^-$ and their six-membered analogues $(\mathbf{6-c})^{\text{Mes}}/[(\mathbf{6-c}')^{\text{Mes}}]^-$, with the smaller change on further ring expansion to $(\mathbf{7-c})^{\text{Mes}}/[(\mathbf{7-c}')^{\text{Mes}}]^-$, reflecting the puckered nature of the seven-membered heterocycle and the consequently smaller effect on the N-C-N angle brought about by the inclusion of the additional backbone methylene spacer.^{4a} The relative effect of the thf dielectric is minimal for the NHC systems, but understandably more pronounced for the negatively charged WCA-NHC and boryl systems, particularly for the latter class of compound in which the negative charge is localized on the low-valent boron centre.

Benzannulated systems $(\mathbf{B-c})^{\text{Mes}}$ and $[(\mathbf{B-b})^{\text{Mes}}]^-$ do not appear to fit easily into the simple trend identified for other NHC/boryl ligands based on the variation in the respective N-E-N angles. Consi-

Table 2 Key orbital energies and compositions (in vacuum and thf dielectric) for the NHCs, WCA-NHCs and boryl ligands depicted in Figure 1.

	Calcd N-E-N angle ($^\circ$)	E(σ) vacuum (thf)	E(p_π) vacuum (thf)	ΔE vacuum (thf)	s:p ratio for HOMO
$(\mathbf{I-c})^{\text{Mes}}$	101.2	-475 (-538)	-33 (-41)	442 (482)	0.71 (0.60)
$(\mathbf{B-c})^{\text{Mes}}$	102.7	-489 (-549)	-15 (-39)	474 (510)	0.68 (0.58)
$(\mathbf{5-c})^{\text{Mes}}$	105.8	-463 (-517)	-33 (-56)	430 (461)	0.60 (0.49)
$(\mathbf{6-c})^{\text{Mes}}$	115.3	-421 (-473)	-42 (-55)	379 (418)	0.56 (0.46)
$(\mathbf{7-c})^{\text{Mes}}$	117.5	-403 (-446)	-52 (-63)	351 (383)	0.54 (0.44)
$[(\mathbf{I-b})^{\text{Mes}}]^-$	97.7	93 (-266)	415 (51)	322 (317)	0.75 (0.66)
$[(\mathbf{B-b})^{\text{Mes}}]^-$	98.1	66 (-283)	393 (60)	327 (343)	0.84 (0.71)
$[(\mathbf{5-b})^{\text{Mes}}]^-$	101.5	94 (-254)	422 (45)	328 (299)	0.61 (0.53)
$[(\mathbf{I-c}')^{\text{Mes}}]^-$	101.3	-231 (-482)	205 (-1)	436 (481)	0.64 (0.48)
$[(\mathbf{5-c}')^{\text{Mes}}]^-$	105.5	-242 (-471)	186 (-6)	428 (465)	0.55 (0.47)
$[(\mathbf{6-c}')^{\text{Mes}}]^-$	114.9	-209 (-429)	182 (-2)	391 (427)	0.52 (0.44)
$[(\mathbf{7-c}')^{\text{Mes}}]^-$	118.4	-194 (-392)	165 (-14)	359 (378)	0.52 (0.43)

-deration of the bond order (and hence length) of the backbone C-C linker, accounts for the N-C-N and N-B-N angles for these benzannulated ligands, which are found to be intermediate between $(\mathbf{I-c})^{\text{Mes}}/[(\mathbf{I-b})^{\text{Mes}}]^-$ (C=C backbone) and $(\mathbf{5-c})^{\text{Mes}}/[(\mathbf{5-b})^{\text{Mes}}]^-$ (C-C backbone). On this basis, it might be expected that the σ orbital energies for both $(\mathbf{B-c})^{\text{Mes}}$ and $[(\mathbf{B-b})^{\text{Mes}}]^-$ would lie between those for the respective saturated/unsaturated systems. However, both ligands feature HOMO (σ) orbitals which are significantly more stabilized (and higher in s-character) than would be expected on the basis of these simple geometric considerations. The additional factor underlying these data is the electron-withdrawing effect of the benzene backbone function in $(\mathbf{B-c})^{\text{Mes}}/[(\mathbf{B-b})^{\text{Mes}}]^-$ - a factor which has been demonstrated elegantly for a range of (poly)aromatic backbone functionalized NHCs by Peris and co-workers.^{18a} This effect is not limited to directly benzannulated heterocycles. Studies of NHC ligands **1** and **2** show that - despite possessing essentially identical (calculated) N-C-N angles (101.2 and 101.7° , respectively; Figure 3)^{18b} - these ligands have Tolman Electronic Parameters (TEPs) of 2046.8

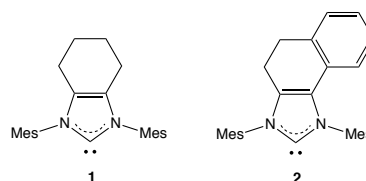


Figure 3 Known NHC systems offering a probe of the electronic effects of benzannulation remote from the carbene centre.^{18b}

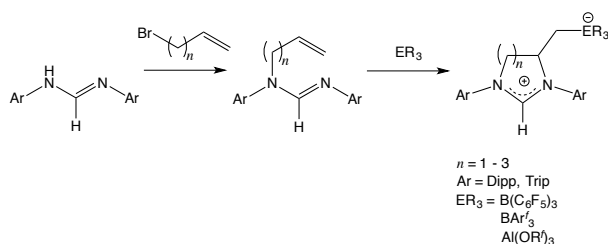
and 2048.0 cm^{-1} ,^{18b} which implies that **2** is a less strongly donating NHC than **1**. The mild electron withdrawing capabilities of the pendant benzene ring in **2** are also consistent with HOMO energies for **1** and **2** (calculated using our method) of -455 and -474 kJ mol^{-1} , respectively.

In a broader sense, examination of the electronic effects of a range of backbone substituents shows (not unexpectedly) that the HOMO energy correlates well with the respective Hammett parameter σ_p (see ESI).²⁰ However, while these initial calculations allow some trends to be identified within a given ligand class, the desired comparison between NHCs on the one hand, and WCA-NHC/boryl donors on the other (e.g. between $(\text{I-c})^{\text{Mes}}$ and $[(\text{I-c}')^{\text{Mes}}]^-$ or $[(\text{I-b})^{\text{Mes}}]^-$), is more difficult to achieve for the ligands in isolation owing to the differences in net charge. With this in mind, we wanted to compare the properties of the different ligands within a family of (otherwise identical) transition metal complexes. Linear Au(I) complexes of the type $[\text{LAuCl}]^{n-}$ (NHC: $n = 0$; WCA-NHC, boryl: $n = 1$) were thought to be good potential model systems, given (i) their geometric simplicity (and the lack of potential complicating effects associated, for example, with the presence of *cis* ligands), and (ii) the large pool of available structural data associated with complexes of this type reported in the literature featuring $\text{L} = \text{NHC}$.²¹ Our experimental efforts were therefore focused on the synthesis and structural characterization of a range of related compounds featuring $\text{L} = \text{WCA-NHC}$ or boryl ligands, in order to allow for direct structural comparisons.

(ii) Experimental and computational studies of gold(I) complexes

Synthetic studies: WCA-NHC complexes

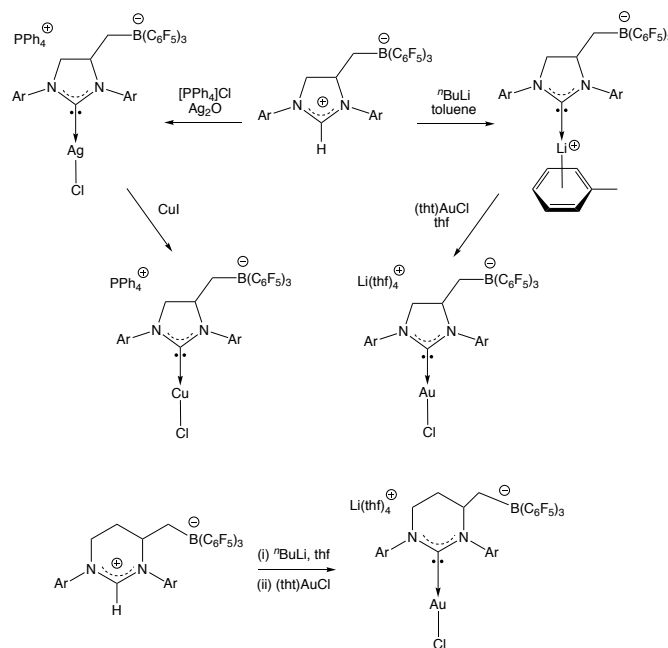
We have recently reported a simple synthetic route to zwitterionic WCA-NHC precursors from formamidine starting materials,⁸ and show herein that this approach can be employed to access not only pro-ligands of varying heterocycle ring sizes, but also systems bearing modified *N*-aryl substituents and a range of backbone tethered borate and aluminate functions (Scheme 1 and ESI).



Scheme 1 Scope of synthetic route to zwitterionic WCA-NHC pro-ligands [where $\text{Ar}^f = \text{C}_6\text{H}_3(\text{CF}_3)_2\text{-}3,5$ and $\text{R}^f = \text{C}(\text{CF}_3)_3$].

Taking the 5-membered heterocycle $\text{H}(\text{5-c}')^{\text{Dipp}}$ as an exemplar, we could subsequently develop routes to the target gold(I) complexes and their congeners featuring the lighter group 11 elements. Thus, straightforward deprotonation at the C(2) position can be effected using *n*-butyllithium in various solvents, with the product of the reaction in toluene solution being confirmed as $(\eta^6\text{-toluene})\text{Li}[(\text{5-c}')^{\text{Dipp}}]$ by a combination of spectroscopic and

crystallographic means (Scheme 2 and Figure 4). A convenient route to group 11 complexes then involves transmetalation from lithium, for example utilizing $(\text{tht})\text{AuCl}$ as a gold(I) precursor. If the reaction is carried out in thf the desired ion pair $[\text{Li}(\text{thf})_4][(\text{5-c}')^{\text{Dipp}}\text{AuCl}]$ is formed in good yield (ca. 60-70%; Scheme 2 and Figure 4).²² In a similar fashion, the anionic complex $[(\text{6-c}')^{\text{Dipp}}\text{AuCl}]^-$ can be generated from the corresponding 6-membered heterocycle via lithiation/trans-metalation onto gold in thf, and isolated either as the $[\text{Li}(\text{thf})_4]^+$ or $[\text{PPN}]^+$ salt (Scheme 2 and Figure 4).



Scheme 2 Syntheses of $\text{M}(\text{I})$ complexes of the group 11 metals of the type $[(\text{WCA-NHC})\text{MCl}]$.

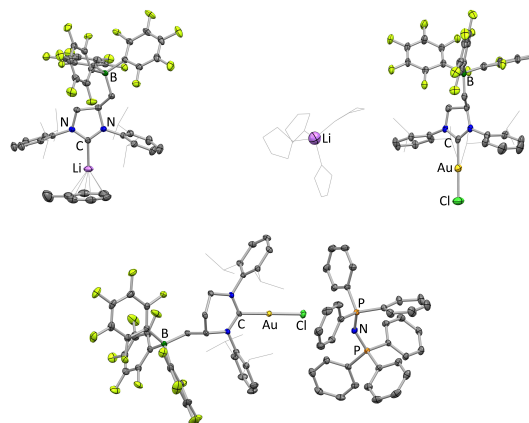


Figure 4 Molecular structures of $(\eta^6\text{-toluene})\text{Li}[(\text{5-c}')^{\text{Dipp}}]$, $[\text{Li}(\text{thf})_4][(\text{5-c}')^{\text{Dipp}}\text{AuCl}]$ and $[\text{PPN}][(\text{6-c}')^{\text{Dipp}}\text{AuCl}]$ as determined by X-ray crystallography. Isopropyl groups and thf molecules shown in wireframe format and hydrogen atoms omitted for clarity; thermal ellipsoids shown at the 35% probability level. Key bond lengths and angles for $(\eta^6\text{-toluene})[(\text{5-c}')^{\text{Dipp}}]$: $d(\text{C-N})$ 1.338(3), 1.342(4), $d(\text{C-Li})$ 2.050(6), $\angle(\text{N-C-N})$ 107.4(2). For structural metrics for gold(I) compounds see Table 3.

Alternatively, following well-established synthetic protocols in NHC chemistry,²³ the direct reaction of $\text{H}(\text{5-c}')^{\text{Dipp}}$ with silver(I) oxide under aerobic conditions (in the presence of a dichloromethane-

soluble chloride source) can be exploited to generate the silver(I) salt $[\text{PPh}_4][(\mathbf{5-c'})^{\text{Dipp}}\text{AgCl}]$, which has also been structurally characterized, and which proves to be a useful transmetalation reagent in its own right – for example in the synthesis of the copper(I) complex $[\text{PPh}_4][(\mathbf{5-c'})^{\text{Dipp}}\text{CuCl}]$ (Scheme 2 and Figure 5).

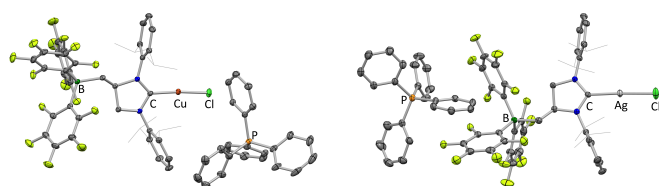
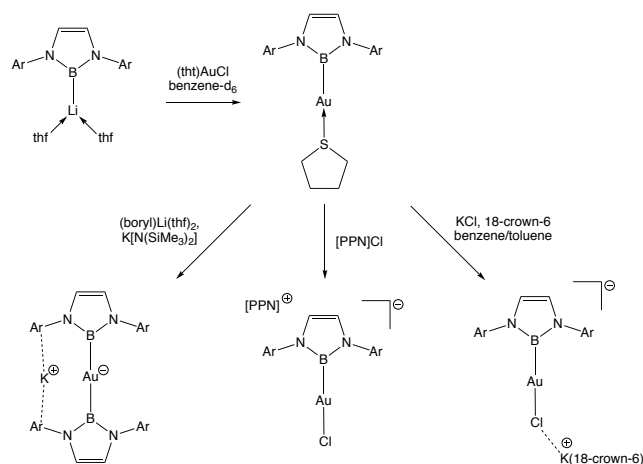


Figure 5 Molecular structures of $[\text{PPh}_4][(\mathbf{5-c'})^{\text{Dipp}}\text{CuCl}]$ and $[\text{PPh}_4][(\mathbf{5-c'})^{\text{Dipp}}\text{AgCl}]$ as determined by X-ray crystallography. Isopropyl groups shown in wireframe format and hydrogen atoms omitted for clarity; thermal ellipsoids shown at the 35% probability level. For key bond lengths and angles see Table 3.

Synthetic studies: boryl complexes

Related synthetic protocols allow access to the targeted boryl complexes of gold(I) (Scheme 3). Thus, a key intermediate of the type $(\mathbf{I-b})^{\text{Dipp}}\text{Au}(\text{tht})$ can be accessed via the direct reaction of $(\text{tht})\text{AuCl}$ with Yamashita's boryllithium reagent $(\text{thf})_2\text{Li}[(\mathbf{I-b})^{\text{Dipp}}]$,¹¹



Scheme 3 Syntheses of novel boryl complexes of Au(I).

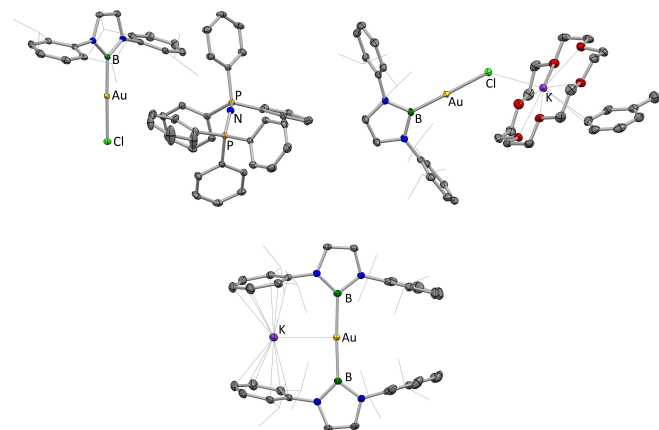


Figure 6 Molecular structures of $[\text{PPN}][(\mathbf{I-b})^{\text{Dipp}}\text{AuCl}]$, $[\text{K}(18\text{-crown-6})][(\mathbf{I-b})^{\text{Dipp}}\text{AuCl}]$ and $\text{K}[(\mathbf{I-b})^{\text{Dipp}}_2\text{Au}]$ as determined by X-ray crystallography. Isopropyl groups shown in wireframe format and hydrogen

atoms omitted for clarity; thermal ellipsoids shown at the 35% probability level. For key bond lengths and angles see Table 4.

and used as a precursor to access both the target chloride ligated species $[(\mathbf{I-b})^{\text{Dipp}}\text{AuCl}]^-$ and the homoleptic complex $[(\mathbf{I-b})^{\text{Dipp}}_2\text{Au}]^-$. In the case of systems containing the $[(\mathbf{I-b})^{\text{Dipp}}\text{AuCl}]^-$ anion, the identity of the counter-cation is shown by crystallographic studies to be potentially important in structural terms, with the $[\text{K}(18\text{-crown-6})]^+$ salt (but not the $[\text{PPN}]^+$ derivative) featuring short contacts between the cation and the gold-bound chloride (Figure 6).

Analysis of experimental structural data

Key structural data derived from the solid-state structures of these novel WCA-NHC and boryl complexes, together with literature data for their NHC analogues, are collated in Tables 3 and 4. For the WCA-NHC complexes, these data are consistent with the idea that their electronic properties are generally similar to those of their 'simple' NHC counterparts – in line with the hypothesis that the anionic component is effectively isolated from the heterocycle via the saturated CH_2 linker. Thus, while the Au-C distance measured for $[(\mathbf{5-c'})^{\text{Dipp}}\text{AuCl}]^-$ is slightly longer than that reported for $(\mathbf{5-c})^{\text{Dipp}}\text{AuCl}$, the *trans* Au-Cl bond length, and both Au-C/Cl distances measured for $[(\mathbf{6-c'})^{\text{Dipp}}\text{AuCl}]^-$ are statistically identical to their simple NHC counterparts. As regards the lighter group 11 congeners, the M-C and M-Cl distances measured for $[(\mathbf{5-c'})^{\text{Dipp}}\text{CuCl}]^-$ and $[(\mathbf{5-c'})^{\text{Dipp}}\text{AgCl}]^-$ are in line with the trends expected based on the covalent radii of the group 11 metals (Cu: 1.38, Ag: 1.53; Au 1.44 Å),¹⁷ and here too, spectroscopic and structural studies of $[\text{PPh}_4][(\mathbf{5-c'})^{\text{Dipp}}\text{AgCl}]$ reveal close similarities with the charge neutral system $(\mathbf{5-c})^{\text{Dipp}}\text{AgCl}$. Thus, the Ag-C and Ag-Cl distances are similar in each case [2.067(3)/2.081(9) and 2.314(1)/2.320(2) Å, respectively], as are the chemical shift and coupling constant data determined from ^{13}C NMR measurements [$\delta_{\text{C}} = 205.1$ ppm, $^1J_{\text{AgC}} = 262/227$ Hz, cf. 207.7 ppm and 253/219 Hz for $(\mathbf{5-c})\text{AgCl}$].²³

As an aside, the availability of structural data for both $[(\mathbf{5-c'})^{\text{Dipp}}\text{AuCl}]^-$ and $[(\mathbf{6-c'})^{\text{Dipp}}\text{AuCl}]^-$ additionally allows the *steric* profiles of these two WCA-NHC systems to be compared with those previously determined for NHCs $(\mathbf{5-c})^{\text{Dipp}}$ and $(\mathbf{6-c})^{\text{Dipp}}$. Given the torsional flexibility of the methylene tether – and the consequent ability of the large borate function to position itself away from the flanking N-bound aryl groups – it is perhaps unsurprising that the percentage buried volumes vary little from those measured for the

Table 3 Key structural parameters relating to group 11 metal complexes containing the WCA-NHC ligands $[(\mathbf{5-c'})^{\text{Dipp}}]$ and $[(\mathbf{6-c'})^{\text{Dipp}}]$, together with comparative literature data for related NHC adducts.

	$d(\text{M-C})$ (Å)	$d(\text{M-Cl})$ (Å)	$\angle(\text{C-M-Cl})$ (°)
$[(\mathbf{5-c'})^{\text{Dipp}}\text{AuCl}]^-$	2.006(5)	2.276(2)	179.7(1)
$[(\mathbf{6-c'})^{\text{Dipp}}\text{AuCl}]^-$	2.011(2)	2.286(1)	178.8(1)
$(\mathbf{5-c'})^{\text{Dipp}}\text{Au}(\text{tht})$	2.012(4)	2.304(2)	172.3(1)
$[(\mathbf{5-c'})^{\text{Dipp}}\text{AgCl}]^-$	2.067(3)	2.314(1)	177.1(1)
$[(\mathbf{5-c'})^{\text{Dipp}}\text{CuCl}]^-$	1.882(2)	2.102(1)	173.9(1)
$(\mathbf{I-c})^{\text{Dipp}}\text{AuCl}$ ²⁴	1.942(3)	2.270(1)	177.0(4)
$(\mathbf{5-c})^{\text{Dipp}}\text{AuCl}$ ²⁵	1.979(3)	2.276(1)	180
$(\mathbf{6-c})^{\text{Dipp}}\text{AuCl}$ ²⁶	2.004(8)	2.281(12)	175.6(3)
$(\mathbf{7-c})^{\text{Dipp}}\text{AuCl}$ ^{4e}	2.012(6)	2.305(1)	178.0(2)
$(\mathbf{5-c})^{\text{Dipp}}\text{AgCl}$ ²³	2.081(9)	2.320(2)	173.7(1)

'simple' NHCs. Thus, the values of % V_{bur} determined from the respective gold(I) chloride complexes are 47.0/47.6 for **(5-c)**^{Dipp} and **[(5-c')^{Dipp}]**, and 50.4/50.8% for **(6-c)**^{Dipp} and **[(6-c')^{Dipp}]**.^{4e,25,28} As such, both steric and electronic data for these WCA-NHCs are consistent with the idea that the backbone WCA function can be incorporated (and provide a marked variation in solubility) while offering minimal perturbation of the key ligand properties at the metal centre.

Table 4 Key structural parameters relating to gold(I) complexes featuring boryl ligand **[(I-b)^{Dipp}]**, together with comparative literature data.

	<i>d</i> (M-B) (Å)	<i>d</i> (M-X) (Å)	\angle (B-M-X) (°)
[(I-b)^{Dipp}AuCl]⁺ ^a	2.040(3)	2.400(1)	176.4(1)
[(I-b)^{Dipp}AuCl]⁺ ^b	2.026(3)	2.405(1)	178.9(1)
[(I-b)^{Dipp}]₂Au⁺	2.139(2), 2.146(2)		176.3(1)
(I-b)^{Dipp}Au(IMes)⁺ ²⁶	2.074(4)	2.078(4)	179.4(2)
(I-b)^{Dipp}Au(PPh₃)⁺ ²⁶	2.076(6)	2.347(1)	172.8(2)
(5-b)^{Dipp}Au(IMes)⁺ ²⁶	2.069(3)	2.070(3)	179.3(1)

^a [PPN]⁺ salt; ^b [K(18-crown)₆](η²-toluene)] salt.

The structural data for the isoelectronic boryl systems (Table 4) can be analysed in a similar fashion. At a general level the Au-B bond lengths determined for all systems are longer than the corresponding NHC Au-C distances, reflecting the larger covalent radius of boron over carbon ($\Delta r = 0.08$ Å). More revealingly, the *trans* Au-Cl bond in the **[(I-b)^{Dipp}AuCl]⁺** system is very much longer [at 2.400(1) Å] than the corresponding linkage in any of the gold(I) NHC complexes listed in Table 3 [longest 2.305(1) Å], and ca. 6% longer than that measured for the directly comparable complex **(I-c)^{Dipp}AuCl**.²⁴ Broader comparison of the *trans* influence of the boryl ligand within a series of Au(I) systems can be carried out by reference to the Au-B distances measured for the homoleptic bis(boryl) complex **[(I-b)^{Dipp}]₂Au⁺** [2.139(2), 2.146(2) Å]. These are put in context by the corresponding (significantly shorter) Au-B bond lengths determined for the same boryl ligand in heteroleptic phosphine, NHC and chloride complexes of the type LAu(boryl) [2.076(6), 2.074(4) and 2.040(3) Å, respectively],²⁷ and imply a *trans* influence series: diazaborolyl >> NHC ≈ tertiary phosphine > Cl[−].

Quantum chemical studies

The relative *trans* influences of NHC, WCA-NHC and boryl ligand classes can also be probed by quantum chemical methods for systems of the type [LAuCl]^{*n*−} (*n* = 0, 1). In the first instance, this can be achieved by using the *trans* metal-halogen bond as a structural probe, thereby extending the scope of experimental studies above in a manner similar to that developed by Marder and Lin.^{13a} In the case of boryl and other anionic ligand systems within the coordination sphere of Pt(II), the major factor determining the relative *trans* influences of alkyl, silyl, boryl ligands etc., was shown to be their σ-donor capabilities (albeit with π-acceptor behaviour also shown to have a discernible effect).^{13a} In the current study we additionally employed the ETS-NOCV (Extended Transition State – Natural Orbitals for Chemical Valence) approach to provide a quantitative picture of the *energetics* of chemical bond formation in [LAuCl]^{*n*−} systems. Under the ETS-NOCV

charge and energy decomposition scheme, the deformation density is partitioned into the different components of the chemical bond, i.e. σ, π and δ. The contributions to the total bond energy can then be calculated for each specific orbital interaction between the respective fragments, in this case the NHC/WCA-NHC/diazaborolyl ligand and the [AuCl] moiety.²⁹

Key data relating to the geometry optimizations and ETS-NOCV analyses for the [LAuCl]^{*n*−} systems are summarized in Table 5. In terms of the *trans* Au-Cl bond length, the most obvious trends are associated with the change from NHC/WCA-NHC donors to boryl ligands. In agreement with the experimental data, like-for-like comparison shows that the Au-Cl distance is >0.1 Å longer for the boron-centred donors. This in turn can be related to the enhanced donor capabilities of the anionic boryl ligand class, with the much higher energy of the σ-symmetry frontier orbital (Table 2) leading a significantly larger σ component to the overall interaction energy (Table 5). The π-acceptor properties of the diazaborolyl ligands are shown to be smaller even than those of NHCs, presumably reflecting the much higher energy of the respective p_π orbital in a ligand system bearing a formal negative charge. Differences between the NHC and WCA-NHC systems, as with the experimental data outlined above, are very minor.

Table 5 Calculated geometric parameters and (ETS-NOCV determined) interaction energies for gold complexes of the type [LAuCl]^{*n*−}.

Ligand	Au-E bond length (Å)	Au-Cl bond length (Å)	<i>E</i> _{int} (σ) (kJ mol ^{−1})	<i>E</i> _{int} (π) (kJ mol ^{−1})
(I-c)^{Mes}	1.981	2.296	-174	-51
(5-c)^{Mes}	1.985	2.296	-178	-53
(6-c)^{Mes}	2.008	2.301	-179	-49
(7-c)^{Mes}	2.011	2.302	-180	-51
[(I-b)^{Mes}][−]	2.022	2.423	-267	-35
[(5-b)^{Mes}][−]	2.028	2.426	-274	-37
[(5-c')^{Mes}][−]	1.992	2.313	-187	-49
[(6-c')^{Mes}][−]	2.013	2.318	-188	-45
[(7-c')^{Mes}][−]	2.019	2.318	-189	-46

Comparisons of calculated data within a given ligand class reflect the greater carbon p orbital character in the HOMO as a function of increasing heterocycle ring size (cf. Table 2) – which results in (i) higher σ orbital energy and (slightly) longer *trans* Au-Cl bonds; and (ii) longer Au-C distances associated with the metal-carbene bond itself.^{13a} Finally, comparison of the complexes featuring the saturated backbone NHC **(5-c)^{Dipp}** with its unsaturated counterpart **(I-c)^{Dipp}** show small differences between the two ligands. **(5-c)^{Dipp}** is predicted to be both a (marginally) stronger σ donor and π acceptor than **(I-c)^{Dipp}**, in line with analyses made by Nolan and co-workers to rationalize the similar TEPs for these two ligands.³⁰

Experimental

General synthetic considerations

All manipulations were carried out using standard Schlenk line or dry-box techniques under an atmosphere of argon. Solvents were

degassed by sparging with argon and dried by passing through a column of the appropriate drying agent using a commercially available Braun SPS. NMR spectra were measured in thf-d₈ or CDCl₃ which were dried over molecular sieves and stored under argon in a Teflon valve ampoule. NMR samples were prepared under argon in 5 mm Wilmad 507-PP tubes fitted with J. Young Teflon valves. NMR spectra were measured on Varian Mercury-VX-300 or Bruker AVII-500 spectrometers; ¹H and ¹³C NMR spectra were referenced internally to residual protio-solvent (¹H) or solvent (¹³C) resonances and are reported relative to tetramethylsilane (δ = 0 ppm). ¹¹B and ²⁷Al NMR spectra were referenced with respect to BF₃OEt₂ and [Al(H₂O)₆]³⁺, respectively. Chemical shifts are quoted in δ (ppm) and coupling constants in Hz. Elemental analyses were carried out at London Metropolitan University. The syntheses of (η⁶-toluene)Li[(5-c')^{Dipp}] and all pro-ligands are described in the supporting information. Syntheses of H(5-c')^{Dipp}, H(6-c')^{Dipp} and [Li(thf)₄][(6-c')AuCl], were previously communicated by us;⁸ (thf)₂Li[(I-b)^{Dipp}] was prepared via the literature method.^{10c}

Syntheses of novel compounds

[Li(thf)₄][(5-c')^{Dipp}AuCl]: A solution of (η⁶-toluene)Li[(5-c')^{Dipp}] (1.34 g, 1.32 mmol) in thf (20 mL) was added to a stirred solution of (tht)AuCl (0.430 g, 1.34 mmol) also in thf (20 mL) at 0°C. After warming to room temperature and stirring for 2 h, the suspension was filtered twice through celite and dried *in vacuo*. The dark blue/purple residue was washed with hexane (2 x 10 mL) to yield the product (1.24 g, 65 % yield) as a pale powder. Colourless crystals suitable for X-ray crystallography were obtained by layering a concentrated thf solution with hexane and storage at room temperature in the dark. ¹H NMR (400 MHz, thf-d₈, 298 K): δ_H 7.27 (2H, t, ³J_{HH} = 7.6 Hz, para-CH of Dipp), 7.21-7.09 (4H, m, meta-CH of Dipp), 3.90 (1H, m, NCH), 3.69 (1H, dd, ^{2/3}J_{HH} = 11.7 Hz, NCH₂), 3.58 (8H, m, OCH₂ of thf), 3.55 (1H, overlapping sept, ¹Pr CH of Dipp), 3.42 (1H, dd, ^{2/3}J_{HH} = 10.3 Hz, NCH₂), 3.12 (1H, sept, ³J_{HH} = 6.8 Hz ¹Pr CH of Dipp), 3.03 (1H, sept, ³J_{HH} = 6.9 Hz ¹Pr CH of Dipp), 2.72 (1H, sept, ³J_{HH} = 6.9 Hz ¹Pr CH of Dipp), 2.32 (1H, dd, ^{2/3}J_{HH} = 12.5 Hz, CH₂B), 1.73 (8H, m, CH₂ of thf), 1.41 (9H, overlapping m, ¹Pr CH₃ of Dipp), 1.27 (9H, overlapping m, ¹Pr CH₃ of Dipp), 1.25 (1H, overlapping m, CH₂B), 1.17 (3H, d, ³J_{HH} = 7.0 Hz, ¹Pr CH₃ of Dipp), 1.04 (3H, d, ³J_{HH} = 6.9 Hz, ¹Pr CH₃ of Dipp). ¹³C NMR (101 MHz, thf-d₈, 298 K): δ_C 195.6 (NCAuN), 149.7 (NC of Dipp), 149.2 (dm, ¹J_{CF} = 233.7 Hz, ortho-CF), 148.1 (NC of Dipp), 148.0, 147.6 (ortho-C of Dipp), 139.4 (dm, ¹J_{CF} = 246.8 Hz, para-CF), 137.5 (dm, ¹J_{CF} = 239.6 Hz, meta-CF), 136.6, 134.7 (ortho-C of Dipp), 130.2, 130.0 (para-CH of Dipp), 125.3, 124.8 (meta-CH of Dipp), 70.1 (NCH), 67.6 (OCH₂ of thf), 59.2 (NCH₂), 30.0, 29.8, 29.7, 29.4 (¹Pr CH of Dipp), 26.8, 25.8, 25.3, 25.0, 23.8, 23.7, 23.6, 23.5 (¹Pr CH₃ of Dipp) (CH₂B not observed). ¹¹B NMR (128 MHz, thf-d₈, 298 K): δ_B -15 (s). ¹⁹F NMR (376 MHz, thf-d₈, 298 K): δ_F -130.8 (d, ³J_{FF} = 21.8 Hz, ortho-CF), -164.9 (t, ³J_{FF} = 20.4 Hz, para-CF), -167.6 (m, meta-CF). ⁷Li NMR (thf-d₈, 156 MHz, 298 K): δ_{Li} -0.6 (s).

[PPh₄][(5-c')^{Dipp}AgCl]: Ag₂O (0.379 g, 1.64 mmol), H(5-c')^{Dipp} (1.50 g, 1.64 mmol) and [PPh₄]Cl (0.613 g, 1.64 mmol) were combined in dry dichloromethane (100 mL) in air and refluxed in the dark for 3 d. The crude mixture was filtered through a short pad of celite to remove any unreacted Ag₂O, and volatiles were then removed *in*

vacuo. Recrystallisation from benzene yielded the product as a colourless crystalline solid (1.20 g, 52% yield). Single crystals suitable for X-ray crystallography were obtained by slow cooling of a toluene solution. ¹H NMR (400 MHz, CDCl₃, 298 K): δ_H 7.75 (4H, tm, ³J_{HH} = 7.3 Hz, para-CH of PPh₄⁺), 7.59 (8H, td, ³J_{HH} = 7.9 Hz, ⁴J_{HP} = 3.6 Hz, meta-CH of PPh₄⁺), 7.45 (8H, ddd, ³J_{HP} = 13.0 Hz, ³J_{HH} = 8.3 Hz, ⁴J_{HH} = 1 Hz, ortho-CH of PPh₄⁺), 7.22-6.97 (6H, m, aromatic CH of Dipp), 3.86 (1H, m, NCH), 3.53 (1H, dd, ^{2/3}J_{HH} = 11.0 Hz, NCH₂), 3.46 (1H, overlapping sept, ³J_{HH} = 6.9 Hz, ¹Pr CH of Dipp), 3.29 (1H, dd, ^{2/3}J_{HH} = 10.8 Hz, NCH₂), 3.02 (1H, sept, ³J_{HH} = 6.9 Hz, ¹Pr CH of Dipp), 2.90 (1H, sept, ³J_{HH} = 7.1 Hz, ¹Pr CH of Dipp), 2.63 (1H, sept, ³J_{HH} = 7.0 Hz, ¹Pr CH of Dipp), 2.12 (1H, dd, ^{2/3}J_{HH} = 13.1 Hz, CH₂B), 1.32 (3H, d, ³J_{HH} = 6.7 Hz, ¹Pr CH₃ of Dipp), 1.23 (6H, overlapping m, ¹Pr CH₃ of Dipp), 1.22 (1H, overlapping m, CH₂B), 1.20 (3H, overlapping d, ³J_{HH} = 6.8 Hz, ¹Pr CH₃ of Dipp), 1.10 (9H, m, ¹Pr CH₃ of Dipp), 0.95 (3H, d, ³J_{HH} = 6.8 Hz, ¹Pr CH₃ of Dipp). ¹³C NMR (126 MHz, CDCl₃, 298 K): δ_C 205.1 (d, ¹J_{109Ag/107AgC} = 262/227 Hz, NCAgN), 148.6 (NC of Dipp), 148.1 (dm, ¹J_{CF} = 240.1 Hz, ortho-CF), 147.2 (NC of Dipp), 147.0, 146.7 (ortho-C of Dipp), 137.7 (dm, ¹J_{CF} = 246.1 Hz, para-CF), 136.3 (dm, ¹J_{CF} = 247.1 Hz, meta-CF), 135.8 (d, ⁴J_{CP} = 3.6 Hz, para-CH of PPh₄⁺), 134.2 (d, ²J_{CP} = 10.0 Hz, ortho-CH of PPh₄⁺), 134.0 (ortho-C of Dipp), 130.6 (d, ³J_{CP} = 12.7 Hz, meta-CH of PPh₄⁺), 129.1, 128.9 (para-CH of Dipp), 124.5, 123.9, 123.8 (meta-CH of Dipp), 117.4 (d, ¹J_{CP} = 91.0 Hz, PC of PPh₄⁺), 69.4 (NCH), 58.4 (NCH₂), 28.9, 28.7, 28.6, 28.3 (¹Pr CH of Dipp), 26.8, 25.6, 25.2, 25.0, 24.3, 23.3, 22.9, 22.8 (¹Pr CH₃ of Dipp) (CH₂B not observed). ¹¹B NMR (128 MHz, CDCl₃, 298K): δ_B -15 (s). ¹⁹F NMR (376 MHz, CDCl₃, 298K): δ_F -130.7 (d, ³J_{FF} = 21.8 Hz, ortho-CF), -163.2 (t, ³J_{FF} = 20.4 Hz, para-CF), -166.2 (m, meta-CF). ³¹P NMR (162 MHz, CDCl₃, 298K): δ_P 23.3 (s). Accurate mass ESI-MS (-): calc. 1056.17371, meas. 1056.17566. Elemental microanalysis: calc. for C₇₀H₅₉AgBClF₁₅N₂P: C 60.13%, H 4.25%, N 2.00%; meas. C 60.26%, H 4.49%, N 2.20%.

[PPh₄][(5-c')^{Dipp}CuCl]: [PPh₄][(5-c')^{Dipp}AgCl] (0.10 g, 71.5 μmol) and CuI (0.014g, 71.5 μmol) were combined in dry acetonitrile (10 mL) in air and stirred at room temperature in the dark for 2 d. Volatiles were removed *in vacuo*, and the residue dissolved in dichloromethane and filtered through a short pad of celite; subsequent removal of solvent *in vacuo* yielded the product as a white crystalline solid (0.07 g, 69% yield). Single crystals suitable for X-ray crystallography were obtained by slow cooling of a toluene solution. ¹H NMR (400 MHz, CDCl₃, 298 K): δ_H 7.85 (4H, tm, ³J_{HH} = 7.3 Hz, para-CH of PPh₄⁺), 7.69 (8H, td, ³J_{HH} = 7.9 Hz, ⁴J_{HP} = 3.6 Hz, meta-CH of PPh₄⁺), 7.55 (8H, ddd, ³J_{HP} = 13.0 Hz, ³J_{HH} = 8.3 Hz, ⁴J_{HH} = 1 Hz, ortho-CH of PPh₄⁺), 7.31-7.07 (6H, m, aromatic CH of Dipp), 3.91 (1H, m, NCH), 3.56 (1H, overlapping dd, ^{2/3}J_{HH} = 12.7 Hz, NCH₂), 3.55 (1H, overlapping sept, ¹Pr CH of Dipp), 3.35 (1H, dd, ^{2/3}J_{HH} = 10.5 Hz, NCH₂), 3.12 (1H, sept, ³J_{HH} = 7.00 Hz, ¹Pr CH of Dipp), 3.00 (1H, sept, ³J_{HH} = 6.6 Hz, ¹Pr CH of Dipp), 2.73 (1H, sept, ³J_{HH} = 6.7 Hz, ¹Pr CH of Dipp), 2.18 (1H, dd, ^{2/3}J_{HH} = 12.7 Hz, CH₂B), 1.42 (3H, d, ³J_{HH} = 6.7 Hz, ¹Pr CH₃ of Dipp), 1.33 (6H, overlapping m, ¹Pr CH₃ of Dipp), 1.32 (1H, overlapping m, CH₂B), 1.30 (3H, overlapping d, ³J_{HH} = 6.8 Hz, ¹Pr CH₃ of Dipp), 1.21 (9H, m, ¹Pr CH₃ of Dipp), 1.06 (3H, d, ³J_{HH} = 6.8 Hz, ¹Pr CH₃ of Dipp). ¹³C NMR (126 MHz, CDCl₃, 298 K): δ_C 200.7 (s, NCCuN), 148.7 (NC of Dipp), 148.1 (dm, ¹J_{CF} = 240.7 Hz, ortho-CF), 147.3 (NC of Dipp), 147.1, 146.7 (ortho-C of Dipp), 137.7 (dm, ¹J_{CF} = 244.3 Hz, para-CF), 136.3 (dm, ¹J_{CF} = 245.2 Hz, meta-CF), 135.9 (d, ⁴J_{CP} = 2.7 Hz, para-CH of PPh₄⁺), 135.7 (ortho-C of Dipp), 134.2 (d,

$^2J_{CP} = 11.8$ Hz ortho-CH of PPh_4^+ , 133.8 (ortho-C of Dipp), 130.7 (d, $^3J_{CP} = 12.7$ Hz, meta-CH of PPh_4^+), 129.0, 128.8 (para-CH of Dipp), 124.4, 123.9, 123.8, 123.7 (meta-CH of Dipp), 117.4 (d, $^1J_{CP} = 89.0$ Hz, PC of PPh_4^+), 68.8 (NCH), 58.4 (NCH₂), 28.9, 28.7, 28.6, 28.3 (1Pr CH of Dipp), 26.7, 25.7, 25.3, 25.0, 24.2, 23.2, 22.8, 22.7 (1Pr CH₃ of Dipp) (CH₂B not observed). ^{11}B NMR (128 MHz, $CDCl_3$, 298 K): δ_B -15 (s). ^{19}F NMR (376 MHz, $CDCl_3$, 298 K): δ_F -130.6 (d, $^3J_{FF} = 23.2$ Hz, ortho-CF), -163.3 (t, $^3J_{FF} = 20.4$ Hz, para-CF), -166.3 (m, meta-CF). ^{31}P NMR (162 MHz, $CDCl_3$, 298 K): δ_P 23.3 (s). Accurate mass ESI-MS (-): calc. 1013.19458, meas. 1013.19645 Elemental microanalysis: calc. for $C_{70}H_{59}CuBClF_{15}N_2P$: C 62.09%, H 4.39%, N 2.07%; meas. C 62.09%, H 4.49%, N 2.16%.

(I-b)^{Dipp}Au(tht): A solution of (thf)₂Li[(I-b)^{Dipp}] (0.051 g, 0.095 mmol) in benzene-d₆ (0.3 mL) was added to suspension of AuCl(tht) (0.030 g, 0.095 mmol) also in benzene-d₆ (0.2 mL), and the reaction mixture turned pale brown with a black precipitate being formed (the colour did not change after storing overnight and no metallic precipitate appeared on the walls). *In situ* 1H NMR monitoring was consistent with high-yielding formation of a gold boryl product, with a small amount of hydroborane and only a trace of chloroborane being formed. The mixture was transferred into a crystallisation tube, volatiles removed *in vacuo* and the residue extracted with hexane. Slow evaporation of solvent at room temperature produced large almost colourless blocks of (I-b)^{Dipp}Au(tht) (0.041 g, 63% yield). 1H NMR (400 MHz, C_6D_6 , 298 K): δ_H 7.18–7.30 (m, 6H, para- and meta-CH of Dipp), 6.41 (s, 2H, NCH), 3.59 (sept, $^3J_{HH} = 6.9$ Hz, 4H, 1Pr CH of Dipp), 2.13 (br t, 4H, SCH₂ of tht), 1.53 (d, $^3J_{HH} = 6.9$ Hz, 12H, 1Pr CH₃ of Dipp), 1.33 (d, $^3J_{HH} = 6.9$ Hz, 12H, 1Pr CH₃ of Dipp), 1.04 (br t, 4H, CH₂ of tht). ^{13}C NMR (126 MHz, C_6D_6 , 298 K): δ_C 146.9 (ortho-C of Dipp), 142.6 (ipso-C of Dipp), 126.9 (para-CH of Dipp), 123.1 (meta-CH of Dipp), 119.8 (NCH), 36.1 (SCH₂ of tht), 30.2 (CH₂ of tht), 28.6 (1Pr CH of Dipp), 25.4 (1Pr CH₃ of Dipp), 24.4 (1Pr CH₃ of Dipp). ^{11}B NMR (128 MHz, C_6D_6 , 298K): δ_B 33 (br s). Elemental microanalysis: calc. for $C_{30}H_{44}AuBN_2S$: C 53.58%, H 6.59%, N 4.17%; meas. C 53.84%, H 6.96%, N 4.15%.

[K(18-crown-6)(η^2 -toluene)][(I-b)^{Dipp}AuCl] and [PPN][(I-b)^{Dipp}AuCl]: Initial attempts to prepare the [(I-b)^{Dipp}AuCl]⁻ anion from (I-b)^{Dipp}Au(tht) by sonicating the tht complex with pre-dried crystalline KCl with 18-crown-6 in thf failed. Instead, the KCl/crown ether adduct was prepared *in situ*: solid KCH₂Ph (0.006 g, 0.046 mmol) was added to a solution of 18-crown-6 (0.014 g, 0.053 mmol) in benzene-d₆ (0.5 mL) in a J. Young's NMR tube. Most of potassium benzyl dissolved upon shaking the tube; solid [Et₃NH]Cl (0.007 g, 0.051 mmol) was then added and the mixture sonicated for ca. 10 min until the orange colour disappeared. To this mixture was added solid (I-b)^{Dipp}Au(tht) (0.022 g, 0.033 mmol). *In situ* 1H NMR monitoring showed that substitution of the tht ligand was incomplete at this point, and in order to drive the reaction, volatiles (including free tht) were removed *in vacuo*. The resulting solid was washed with hexane and dried *in vacuo*, with NMR monitoring showing that the new product had been formed cleanly. After transferral to a crystallisation tube, the residue was dried at 50°C in order to remove benzene apparently coordinated to potassium. Addition of toluene (0.5 mL) resulted in partial dissolution, and the solution was decanted to the second part of the tube and

evaporated to a drop of viscous liquid, which produced several large block-like crystals suitable for X-ray crystallography. 1H NMR (400 MHz, C_6D_6 , 298 K): δ_H 7.15–7.25 (m, 6H, para- and meta-CH of Dipp + C_6D_5H), 6.46 (s, 2H, NCH), 3.79 (sept, $^3J_{HH} = 6.7$ Hz, 4H, 1Pr CH of Dipp), 3.20 (s, 24H, 18-crown-6), 1.57 (d, $^3J_{HH} = 6.7$ Hz, 12H, 1Pr CH₃ of Dipp), 1.38 (d, $^3J_{HH} = 6.7$ Hz, 12H, 1Pr CH₃ of Dipp). ^{13}C NMR was not assigned due to low solubility. ^{11}B NMR (128 MHz, C_6D_6 , 298K): δ_B 31 (br s). [PPN][(I-b)^{Dipp}AuCl]: Solid [PPN]Cl (0.022 g, 0.039 mmol) was added to a solution of (I-b)^{Dipp}Au(tht) (0.026 g, 0.039 mmol) in C_6D_6 (0.5 mL). Copious precipitate was forming around crystals of [PPN]Cl and after sonication a thick suspension was formed (1H NMR showed only small amount of hydroborane in solution). The mixture was transferred into two-legged tube and evaporated to dryness; when Et₂O was added by vacuum transfer the product remained insoluble, thus it was washed by decantation three times and dried yielding lilac powder of [PPN][(I-b)^{Dipp}AuCl] (0.038 g, 84% yield). X-Ray quality colourless crystals (needles) and analytical sample were prepared by layering a dichloromethane solution with hexane and storing at 4 °C. 1H NMR (400 MHz, CD_2Cl_2 , 298 K): δ_H 7.67 (br s, 6H, para-CH of Ph), 7.44–7.52 (m, 24H, ortho- and meta-CH of Ph), 7.24 (t, $^3J_{HH} = 7.5$ Hz, 2H, para-CH of Dipp), 7.17 (d, $^3J_{HH} = 7.5$ Hz, 4H, meta-CH of Dipp), 6.19 (s, 2H, NCH), 3.29 (sept, $^3J_{HH} = 6.7$ Hz, 4H, 1Pr CH of Dipp), 1.31 (d, $^3J_{HH} = 6.7$ Hz, 12H, 1Pr CH₃ of Dipp), 1.17 (d, $^3J_{HH} = 6.7$ Hz, 12H, 1Pr CH₃ of Dipp). ^{13}C NMR (126 MHz, CD_2Cl_2 , 298 K): δ_C 146.6 (ortho-C of Dipp), 142.9 (ipso-C of Dipp), 133.6 (para-CH of Ph), 131.9 (ortho-CH of Ph), 129.3 (meta-CH of Ph), 126.8 (d, $^1J_{CP} = 109.7$ Hz, ipso-C of Ph), 125.5 (para-CH of Dipp), 122.4 (meta-CH of Dipp), 118.4 (NCH), 27.9 (1Pr CH of Dipp), 24.4 (1Pr CH₃ of Dipp), 23.7 (1Pr CH₃ of Dipp). ^{11}B NMR (128 MHz, CD_2Cl_2 , 298K): δ_B 31 (br s). ^{31}P NMR (162 MHz, CD_2Cl_2 , 298K): 21.0 (s). Elemental microanalysis: calc. for $C_{62}H_{66}AuBClN_3P_2$: C 64.29%, H 5.74%, N 3.63%; meas. C 63.92%, H 5.93%, N 3.81%.

K[(I-b)^{Dipp}2Au]: Solid (thf)₂Li[(I-b)^{Dipp}] (0.15 g, 0.027 mmol) was added to a solution of (I-b)^{Dipp}Au(tht) (0.019 g, 0.027 mmol) in benzene-d₆ (0.5 mL). *In situ* monitoring by 1H NMR showed the formation of a single new product. Solid K[N(SiMe₃)₂] (0.006 g, 0.027 mmol) was then added (to sequester the Li⁺ as Li[N(SiMe₃)₂]) and again a new single boryl-containing product was formed. Volatiles were removed *in vacuo* at room temperature and the resulting residue extracted with several portions of hexane. Crystallization by slow evaporation at room temperature yielded colourless plates of K[(I-b)^{Dipp}2Au] (0.023 g, 84% yield). 1H NMR (400 MHz, C_6D_6 , 298 K): δ_H 6.98–7.09 (m, 12H, para- and meta-CH of Dipp), 6.27 (s, 4H, NCH), 3.45 (sept, $^3J_{HH} = 6.8$ Hz, 8H, 1Pr CH of Dipp), 1.18 (br pseudo triplet, 48H, 1Pr CH₃ of Dipp). ^{13}C NMR (126 MHz, C_6D_6 , 298 K): δ_C 147.8 (ortho-C of Dipp), 145.2 (ipso-C of Dipp), 126.1 (para-CH of Dipp), 123.0 (meta-CH of Dipp), 119.4 (NCH), 28.5 (1Pr CH of Dipp), 24.9 (1Pr CH₃ of Dipp), 24.0 (1Pr CH₃ of Dipp). ^{11}B NMR (128 MHz, C_6D_6 , 298K): δ_B 68 (br s). Reliable elemental microanalysis proved impossible to obtain for this highly air- and moisture-sensitive compound

Computational approach

DFT calculations, including geometry optimization, fragment calculation and ETS-NOCV (extended transition state-Natural Orbitals for Chemical Valence) were performed using the Amsterdam Density Functional (ADF) 2014 software package.

Calculations were performed using the Vosko-Wilk-Nusair local density approximation with exchange from Becke,³¹ and correlation correction from Perdew,³² and 3-dimensional dispersion effect (BP86-D3).³³ Slater-type orbitals (STOs)³⁴ were used for the triple zeta basis set with an additional set of polarization functions (TZP).³⁵ The full-electron basis set approximation was applied with no molecular symmetry. General numerical quality was good. Geometric details and molecular orbital energies were obtained after unrestricted geometry optimization; the energies of interaction between fragments were recorded after fragment calculation using the ETS-NOCV approach.²⁹

Crystallography

Diffraction data for $(\eta^6\text{-toluene})\text{Li}[(5\text{-c'})^{\text{Dipp}}]$, $[\text{Li}(\text{thf})_4][[(5\text{-c'})^{\text{Dipp}}\text{AuCl}]$, $[\text{PPN}][[(6\text{-c'})^{\text{Dipp}}\text{AuCl}]$, $(5\text{-c'})^{\text{Dipp}}\text{Au}(\text{tht})$, $[\text{PPh}_4][[(5\text{-c'})^{\text{Dipp}}\text{CuCl}]$, $[\text{PPh}_4][[(5\text{-c'})^{\text{Dipp}}\text{AgCl}]$, $[\text{PPN}][[(\text{I-b})^{\text{Dipp}}\text{AuCl}]$, $[\text{K}(\text{18-crown-6})(\eta^2\text{-toluene})][[(\text{I-b})^{\text{Dipp}}\text{AuCl}]$ and $[\text{K}[(\text{I-b})^{\text{Dipp}}_2\text{Au}]$ were collected using an Oxford Diffraction (Agilent) SuperNova diffractometer at 150 K; data were reduced using DENZO, SCALEPACK or CrysAlisPro, and the structures were solved with either SuperFlip or SHELXT and refined with full-matrix least squares within CRYSTALS or SHELXL-2014, as described in the CIF.³⁶ Complete details of the X-ray analyses have been deposited at The Cambridge Crystallographic Data Centre (CCDC 1838444-1838456).

Conclusions

A combination of quantum chemical and experimental approaches has been employed to probe electronic structure in two series of anionic ligands related to the well-known N-heterocyclic carbene (NHC) class of donor, viz NHC ligands incorporating a pendant weakly coordinating anion (WCA-NHCs), and isoelectronic (formally anionic) diazaborolyl systems. Computational analyses (i) of the respective frontier orbital energies/compositions for the 'free' ligands and (ii) of the results of ETS-NOCV studies of the bonding in model group 11 complexes are viewed in the context of the structural metrics determined for novel (linear) gold(I) compounds featuring WCA-NHC or diazaborolyl ligands. Key findings are that the former class of ligand – in which the WCA component is attached to the ligand heterocycle via a methylene (CH_2) spacer – offers electronic (and steric) properties which are largely unperturbed from their 'simple' NHC counterparts, while diazaborolyl donors (in which the negative charge is formally located at the boron donor atom) offer significantly stronger σ -donation and a very high *trans* influence.

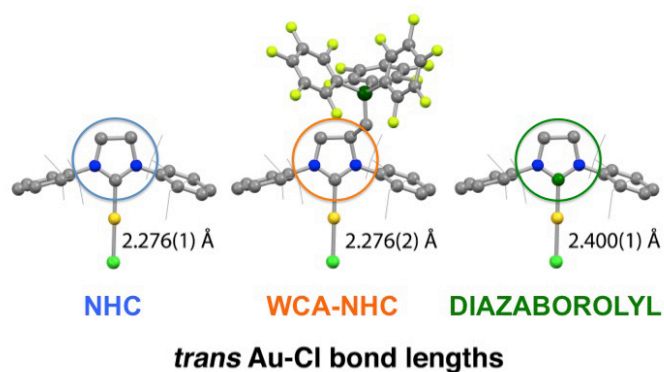
Acknowledgements

We acknowledge funding from the EPSRC (AP, grant number EP/L025000/1), EU Marie Curie program (ELK, grant number PIEF-GA-2013-626441).

Notes and references

- See, for example: (a) A. J. Arduengo, *Acc. Chem. Res.*, 1999, **32**, 913; (b) D. Bourissou, O. Guerret, F. P. Gabbaï and G. Bertrand, *Chem. Rev.*, 2000, **100**, 39; (c) F. E. Hahn and M.C. Jahnke, *Angew. Chem., Int. Ed.*, 2008, **47**, 3122; (d) T. Dröge and F. Glorius, *Angew. Chem., Int. Ed.*, 2010, **49**, 6940; (e) D. Martin, M. Melaimi, M. Soleilhavoup and G. Bertrand, *Organometallics*, 2011, **30**, 5304; (f) M. N. Hopkinson, C. Richter, M. Schedler and F. Glorius, *Nature*, 2014, **510**, 485.
- See, for example: (a) W. A. Herrmann, *Angew. Chem., Int. Ed.*, 2002, **41**, 1290; (b) S. Würtz and F. Glorius, *Acc. Chem. Res.*, 2008, **41**, 1523; (c) R. Corberán, E. Mas-Márza and E. Peris, *Eur. J. Inorg. Chem.*, 2009, 1700; (d) J. C. Y. Lin, R. T. W. Huang, C. S. Lee, A. Bhattacharyya, W. S. Hwang and I. J. B. Lin, *Chem. Rev.*, 2009, **109**, 3561; (e) S. Díez-González, N. Marion and S. P. Nolan, *Chem. Rev.*, 2009, **109**, 3612.
- For a very recent review of electronic structure in carbene complexes, see: D. Munz, *Organometallics*, 2018, **37**, 275.
- (a) M. Iglesias, D. J. Beetstra, J. C. Knight, L. L. Ooi, A. Stasch, S. Coles, L. Male, M. B. Hursthouse, K. J. Cavell, A. Dervisi and I. A. Fallis, *Organometallics*, 2008, **27**, 3279; (b) E. L. Kolychev, I. A. Portnyagin, V. V. Shuntikov, V. N. Khrustalev and M. S. Nechaev, *J. Organomet. Chem.*, 2009, **694**, 2454; (c) M. Iglesias, D. J. Beetstra, B. Kariuki, K. J. Cavell, A. Dervisi and I. A. Fallis, *Eur. J. Inorg. Chem.*, 2009, 1913; (d) S. Flügge, A. Anoop, R. Goddard, W. Thiel and A. Fürstner, *Chem.-Eur. J.*, 2009, **15**, 8558; (e) J. J. Dunsford, K. J. Cavell and B. Kariuki, *Organometallics*, 2012, **31**, 4118.
- For a recent review, see: M. Melaimi, R. Jazzar, M. Soleilhavoup and G. Bertrand, *Angew. Chem., Int. Ed.*, 2017, **56**, 10046.
- (a) A. Wacker, H. Pritzow and W. Siebert, *Eur. J. Inorg. Chem.*, 1998, 843; (b) R. Fränkel, J. Kniczek, W. Ponikwar, H. Nöth, K. Polborn and W. P. Fehlhammer, *Inorg. Chim. Acta*, 2001, **312**, 23; (c) A. Weiss, H. Pritzkow and W. Siebert, *Eur. J. Inorg. Chem.*, 2002, 1607; (d) A. Wacker, C. G. Yan, G. Kaltenpoth, A. Ginsberg, A. M. Arif, R. D. Ernst, H. Pritzkow and W. Siebert, *J. Organomet. Chem.*, 2002, **641**, 195; (e) V. César, N. Lugan and G. Lavigne, *J. Am. Chem. Soc.*, 2008, **130**, 11286; (f) I. V. Shishkov, F. Rominger and P. Hofmann, *Organometallics*, 2009, **28**, 3532; (g) V. César, N. Lugan and G. Lavigne, *Chem. Eur. J.*, 2010, **16**, 11432; (h) J. J. Scepaniak, C. S. Vogel, M. M. Khusniyarov, F. W. Heinemann, K. Meyer and J. M. Smith, *Science*, 2011, **331**, 1049; (i) N. Vujkovic, V. César, N. Lugan and G. Lavigne, *Chem. Eur. J.*, 2011, **17**, 13151.
- (a) S. Kronig, E. Theuergarten, C. G. Daniliuc, P. G. Jones and M. Tamm, *Angew. Chem., Int. Ed.*, 2012, **51**, 3240; (b) E. L. Kolychev, S. Kronig, K. Brandhorst, M. Freytag, P. G. Jones and M. Tamm, *J. Am. Chem. Soc.*, 2013, **135**, 12448; (c) A. Winkler, K. Brandhorst, M. Freytag, P. G. Jones and M. Tamm, *Organometallics*, 2016, **35**, 1160; (d) A. Igarashi, E. L. Kolychev, M. Tamm and K. Nomura, *Organometallics*, 2016, **35**, 1778.
- N. Phillips, R. Tirfoin and S. Aldridge, *Dalton Trans.*, 2014, **43**, 15279.
- S. Onowaza, Y. Hatanaka, T. Sakakura, S. Shimada and M. Tanaka, *Organometallics*, 1996, **15**, 5450.
- For reviews of metal boryl chemistry see, for example: (a) G.J. Irvine, M.J.G. Lesley, T.B. Marder, N.C. Norman, C.R. Rice, E.G. Robins, W.R. Roper, G.R. Whittell and L.J. Wright, *Chem. Rev.*, 1998, **98**, 2685; (b) S. Aldridge and D.L. Coombs, *Coord. Chem. Rev.*, 2004, **248**, 535 (c) D.L. Kays and S. Aldridge,

- Struct. Bonding (Berlin)*, 2008, **130**, 29; (d) L. Dang, Z. Lin and T.B. Marder, *Chem. Commun.*, 2009, 3987; (e) H. Braunschweig, R.D. Dewhurst and A. Schneider, *Chem. Rev.* 2010, **110**, 3924.
- 11 (a) Y. Segawa, M. Yamashita and K. Nozaki, *Science*, 2006, **314**, 113; (b) Y. Segawa, Y. Suzuki, M. Yamashita and K. Nozaki, *J. Am. Chem. Soc.*, 2008, **130**, 16069; (c) M. Yamashita, Y. Suzuki, Y. Segawa and K. Nozaki, *Chem. Lett.*, 2008, **37**, 802. For a very recent review, see: (d) L. Weber, *Eur. J. Inorg. Chem.*, 2017, 3461.
- 12 For an early computational investigation of diazaborolyl systems, see: A. Sundermann, M. Reiher and W. W. Schoeller, *Eur. J. Inorg. Chem.* 1998, 305.
- 13 (a) J. Zhu, Z. Lin and T. B. Marder, *Inorg. Chem.*, 2005, **44**, 9384. See also: (b) A. A. Dickinson, D. J. Willock, R. J. Calder and S. Aldridge, *Organometallics*, 2002, **21**, 1146; (c) K.C. Lam, W. H. Lam, Z. Lin, T. B. Marder and N. C. Norman, *Inorg. Chem.*, 2004, **43**, 2541; (d) H. Braunschweig, K. Radacki, D. Rais and D. Scheschkewitz, *Angew. Chem., Int. Ed.*, 2005, **44**, 5651.
- 14 (a) L. M. A. Saleh, K. H. Birj Kumar, A. V. Protchenko, A. D. Schwarz, S. Aldridge, C. Jones, N. Kaltsoyannis and P. Mountford, *J. Am. Chem. Soc.*, 2011, **133**, 3836; (b) A. V. Protchenko, K. H. Birj Kumar, D. Dange, A. D. Schwarz, D. Vidovic, C. Jones, N. Kaltsoyannis, P. Mountford and S. Aldridge, *J. Am. Chem. Soc.*, 2012, **134**, 6500; (c) A. V. Protchenko, D. Dange, A. D. Schwarz, C. Y. Tang, N. Phillips, P. Mountford, C. Jones and S. Aldridge, *Chem. Commun.*, 2014, **50**, 3841; (d) A. V. Protchenko, D. Dange, J. R. Harmer, C. Y. Tang, A. D. Schwarz, M. J. Kelly, N. Phillips, R. Tirfoin, K. H. Birj Kumar, C. Jones, N. Kaltsoyannis, P. Mountford and S. Aldridge, *Nature Chem.*, 2014, **6**, 315; (e) A. V. Protchenko, D. Dange, M. P. Blake, A. D. Schwarz, C. Jones, P. Mountford and S. Aldridge, *J. Am. Chem. Soc.*, 2014, **136**, 10902; (f) A. V. Protchenko, M. P. Blake, A. D. Schwarz, C. Jones, P. Mountford and S. Aldridge, *Organometallics*, 2015, **34**, 2126; (g) A. V. Protchenko, J. I. Bates, L. M. A. Saleh, M. P. Blake, A. D. Schwarz, E. L. Kolychev, A. L. Thompson, C. Jones, P. Mountford and S. Aldridge, *J. Am. Chem. Soc.*, 2016, **138**, 4555; (h) A. Rit, J. Campos, H. Niu and S. Aldridge, *Nature Chem.*, 2016, **8**, 1022; (i) A. V. Protchenko, J. Urbano, J. A. B. Abdalla, J. Campos, D. Vidovic, A. D. Schwarz, M. P. Blake, P. Mountford, C. Jones and S. Aldridge, *Angew. Chem., Int. Ed.*, 2017, **56**, 15098.
- 15 A. J. Arduengo III, H. V. R. Dias, R. L. Harlow and M. Kline J. *Am. Chem. Soc.*, 1992, **114**, 5530.
- 16 A. J. Arduengo III, J. R. Goerlich and W. J. Marshall, *J. Am. Chem. Soc.*, 1995, **117**, 11027.
- 17 B. Cordero, V. Gómez, A. E. Platero-Prats, M. Revés, J. Echeverría, E. Cremades, F. Barragán and S. Alvarez, *Dalton Trans.*, 2008, 2832.
- 18 (a) H. Valdés, M. Poyatos and E. Peris, *Inorg. Chem.*, 2015, **54**, 3654; (b) S. Urban, M. Tursky, R. Fröhlich and F. Glorius, *Dalton Trans.*, 2009, 6934.
- 19 C. A. Tolman, *Chem. Rev.*, 1977, **77**, 313.
- 20 C. Hansch, A. Leo and R. W. Taft, *Chem. Rev.*, 1991, **91**, 165.
- 21 See, for example, S. P. Nolan, *Acc. Chem. Res.*, 2011, **44**, 91.
- 22 The outcome of this reaction is solvent dependent: the zwitterionic system (5-c')^{Dipp}Au(tht) can be isolated in low yield from the reaction in toluene and characterized crystallographically (ESI).
- 23 P. de Fremont, N. M. Scott, E. D. Stevens, T. Ramnial, O. C. Lightbody, C. L. B. Macdonald, J. A. C. Clyburne, C. D. Abernethy and S. P. Nolan, *Organometallics*, 2005, **24**, 6301.
- 24 M. R. Fructos, T. R. Belderrain, P. de Fremont, N. M. Scott, S. P. Nolan, M. M. Diaz-Requejo and P. J. Perez, *Angew. Chem., Int. Ed.*, 2005, **44**, 5284.
- 25 P. de Fremont, N. M. Scott, E. D. Stevens and S. P. Nolan, *Organometallics*, 2005, **24**, 2411.
- 26 S. Flugge, A. Anoop, R. Goddard, W. Thiel and A. Furstner, *Chem.-Eur. J.*, 2009, **15**, 8558.
- 27 Y. Segawa, M. Yamashita, K. Nozaki, *Angew. Chem., Int. Ed.*, 2007, **46**, 6710.
- 28 %V_{bur}: (a) A. C. Hillier, W. J. Sommer, B. S. Yong, J. L. Petersen, L. Cavallo and S. P. Nolan, *Organometallics*, 2003, **22**, 4322; (b) L. Cavallo, A. Correa, C. Costabile and H. Jacobsen, *J. Organomet. Chem.*, 2005, **690**, 5407; (c) A. Poater, B. Cosenza, A. Correa, S. Giudice, F. Ragone, V. Scarano and L. Cavallo, *Eur. J. Inorg. Chem.*, 2009, 1759; (d) F. Ragone, A. Poater and L. Cavallo, *J. Am. Chem. Soc.*, 2010, **132**, 4249; (e) H. Clavier and S. P. Nolan, *Chem. Commun.*, 2010, **46**, 841; (f) L. Faliuvene, R. Credendino, A. Poater, A. Petta, L. Serra, R. Oliva, V. Scarano and L. Cavallo, *Organometallics*, 2016, **35**, 2286.
- 29 M. P. Mitoraj, A. Michalak and T. Ziegler, *Organometallics*, 2009, **28**, 3727.
- 30 R. A. Kelly, III, H. Clavier, S. Giudice, N. M. Scott, E. D. Stevens, J. Bordner, I. Samardjiev, C. D. Hoff, L. Cavallo and S. P. Nolan, *Organometallics*, 2008, **27**, 202.
- 31 A. D. Becke, *Phys. Rev. A*, 1988, **38**, 3098.
- 32 J. P. Perdew, *Phys. Rev. B*, 1986, **33**, 8822.
- 33 S. Grimme, J. Antony, S. Ehrlich and H. Krieg, *J. Chem. Phys.*, 2010, **132**, 154104.
- 34 J. C. Slater, *Phys. Rev.*, 1930, **36**, 57.
- 35 E. Van Lenthe and E. J. Baerends, *J. Comput. Chem.*, 2003, **24**, 1142.
- 36 (a) Z. Otwinowski, W. Minor. In *Processing of X-Ray Diffraction Data Collected in Oscillation Mode*, *Methods Enzymol.* (C.W. Carter, R.M. Sweet eds.), pp. 307-326. Academic Press, New York (1997); (b) L. Palatinus and G. Chapuis, *J. Appl. Crystallogr.*, 2007, **40**, 786; (c) P.W. Betteridge, J.R. Carruthers, R.I. Cooper, K. Prout and D.J. Watkin, *J. Appl. Cryst.*, 2003, **36**, 1487; (d) R.I. Cooper, A.L. Thompson, D.J. Watkin, *J. Appl. Crystallogr.*, 2010, **43**, 1100; (e) A.L. Thompson and D.J. Watkin, *J. Appl. Crystallogr.*, 2011, **44**, 1017; (f) G. M. Sheldrick, SHELX-2014 package (2014).



A combination of quantum chemical and synthetic/crystallographic methods have been employed to probe electronic structure in two series of anionic ligands related to the well-known NHC donor class: WCA-NHC ligands (featuring a weakly-coordinating anion component appended via a methylene spacer) – offer electronic properties largely unperturbed from their 'simple' NHC counterparts, while diazaborolyl donors offer significantly stronger σ -donation and a very high *trans* influence.